Desalination 527 (2022) 115552

Contents lists available at ScienceDirect

Desalination

journal homepage: www.elsevier.com/locate/desal

Nanofiltration of complex mixtures: The effect of the adsorption of divalent ions on membrane retention

S. Castaño Osorio [a,b], P.M. Biesheuvel [a], J.E. Dykstra [b,*], E. Virga [a,c]

[a] Wetsus, European Centre of Excellence for Sustainable Water Technology, Oostergoweg 9, 8911 MA Leeuwarden, The Netherlands
[b] Environmental Technology, Wageningen University, Bornse Weilanden 9, 6708 WG Wageningen, The Netherlands
[c] Membrane Science and Technology, University of Twente, Drienerlolaan 5, 7522 NB Enschede, The Netherlands

HIGHLIGHTS

- Adsorption of multivalent counterions affects the membrane charge.
- Mean-field theory can accurately predict ion rejection and charge reversal.
- Coupling the Extended Nernst-Planck equation and a Langmuir adsorption model improves model predictions.
- Membrane charge reversal must be considered when multivalent ions are present in solution.

GRAPHICAL ABSTRACT

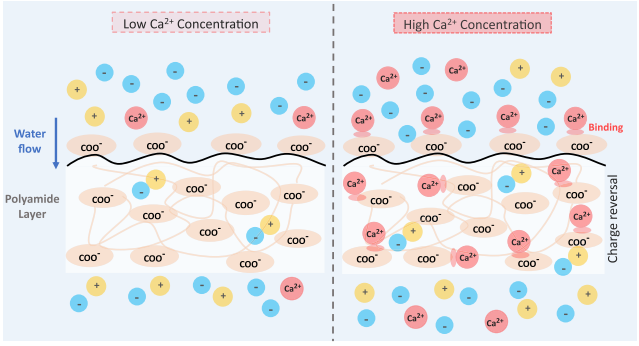

ARTICLE INFO

Keywords:
Nanofiltration
Divalent ion adsorption
Membrane retention

ABSTRACT

In nanofiltration (NF), solution and membrane chemistry determine the membrane charge density. In multi-component electrolytes solutions, it is important to consider the interaction between ions and NF membranes. For instance, in the presence of divalent ions, charge reversal can take place due to the interaction of counterions with the charged functional groups of the membrane. This paper presents a model based on state-of-the-art mean-field theory that includes the effect of divalent counterions on the membrane charge density. By using a Langmuir equation with two model parameters, we consider the adsorption of divalent ions (e.g., Ca^{2+} and Mg^{2+}) in the polyamide active layer of the membrane and calculate the effective membrane charge density. Two different sets of experimental data from literature are used to evaluate the model. Contrary to the statement of a recent study on NF, we show that mean-field theory can predict the rejection of all types of ions in a multi-component electrolyte solution when the effect of divalent counterions on the membrane charge density is included. Moreover, the results in this study reinforce the idea that adsorption of counterions plays a fundamental role in the performance of nanofiltration.

* Corresponding author.
E-mail address: jouke.dykstra@wur.nl (J.E. Dykstra).

https://doi.org/10.1016/j.desal.2022.115552
Received 29 October 2021; Received in revised form 13 December 2021; Accepted 3 January 2022
Available online 28 January 2022

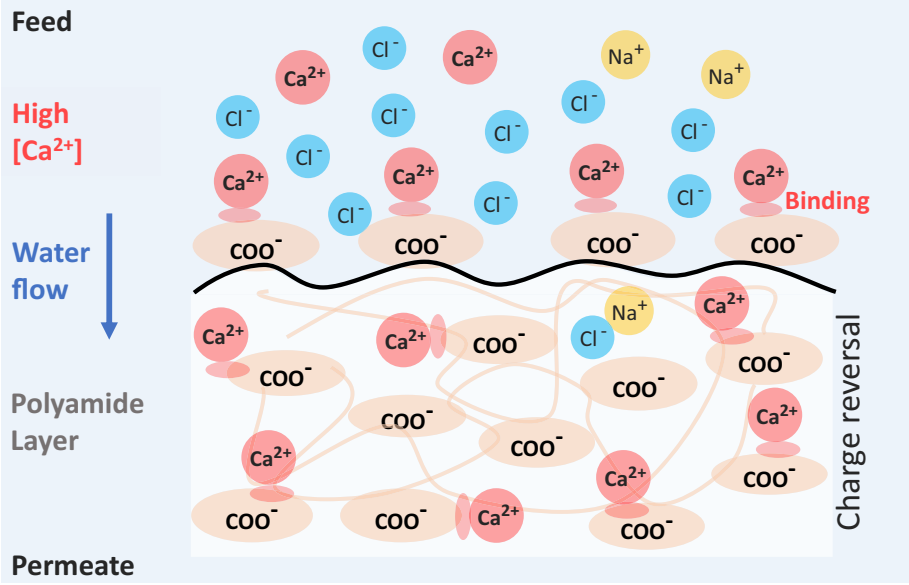

Fig. 1. General illustration of binding between Ca^{2+} ions and the carboxylic groups in a PA top layer of a nanofiltration (NF) membrane. With high enough Ca^{2+} concentration, the net charge of the membrane is reversed from negative to positive.

1. Introduction

In terms of rejection, NF is in between ultrafiltration (UF) and reverse osmosis (RO) [1,2] and presents several advantages compared to these other technologies. For instance, NF requires lower operating pressure and energy consumption than RO, while higher water permeability is achieved. Despite the lower pressure applied, NF can still achieve high retention of multivalent ions and dissolved organic matter [3]. Therefore, NF can be used in different applications such as water reclamation, removal of impurities, and scaling prevention [4–13]. In addition, using NF as pre-treatment for RO improves the overall desalination performance because water recovery increases, energy consumption decreases, and less chemical cleaning is needed.

In desalination, polyamide (PA) thin-film composite (TFC) membranes are the most commonly used because of their high selectivity and permeability [14]. PA-TFC membranes consist typically of a low resistance support layer and a functionally active top layer, which plays the main role in the separation and rejection of ions [15]. The top polyamide layer in these membranes contains carboxylic and amine groups that normally, at neutral or alkaline pH, give a strong negative surface charge to the membrane [16], which also serves to reduce organic fouling [17].

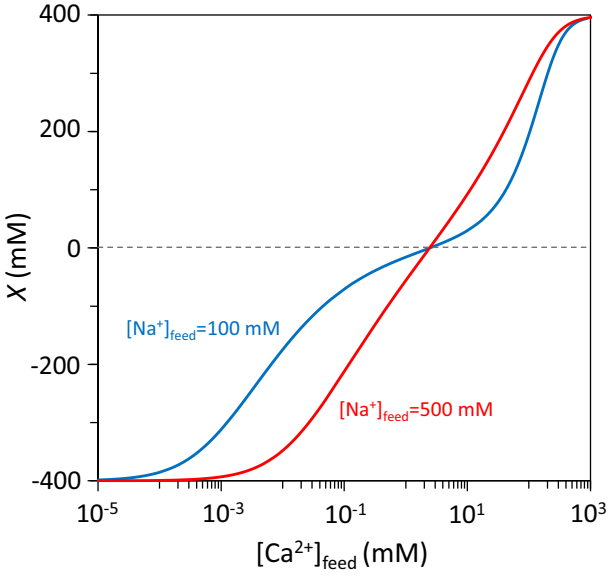

Fig. 2. Membrane charge density as a function of $[Ca^{2+}]_{feed}$ for two solutions with different $[Na^{+}]_{feed}$, 100 mM (blue) and 500 mM (red). Model parameters are given in Table 2, Case I.

During NF operation, the removal of contaminants and ions from water is the consequence of a combination of phenomena, such as steric and Donnan exclusion [17,18]. In addition, other transport effects, such as hindered diffusion in the pores of the membrane, play an important role [19].

We next provide a brief overview of literature on transport theory in NF. The mean-field theory is a modelling approach where physical reality is described using continuum equations, formulated as mass balances and flux equations, based on averaged-out properties such as concentrations, pressures, and various potentials [20]. In NF, the extended Nernst-Planck (ENP) equation, which describes fluxes based on diffusion, advection, and electromigration [21], has been widely used [22–25]. For instance, Peters et al. used the extended Nernst-Planck equation to study the rejection of different single salts and compared their prediction with experimental data [26]. Models based on the ENP equation can be easily extended to include, besides ion transport, physical and chemical phenomena, such as chemical equilibrium of amphoteric ions [27] and acid-base reactions inside the membrane [20,28].

Besides the models based on mean-field theory, phenomenological models that are based on the Nernst-Planck equation have been proposed. For instance, Fridman et al. [29] studied and theoretically described the rejection of prevalent ions in seawater (Cl^{-}, Na^{+}, Ca^{2+}), and concluded that, to accurately predict ion concentrations in the permeate, one has to account for the presence of divalent ions [29]. Bason et al. found that ion adsorption and binding of counterions to the charged groups of an NF membrane can radically affect ion retention, and suggested that it needs to be included for accurate model predictions [30]. Recently, from these phenomenological approaches, objections were raised to the applicability of mean-field theory to describe ion transport and include the interaction between ions and the membrane [31].

In NF with PA-TFC membranes, it is important to consider the interaction between counterions (cations for negatively charged

membranes) and functional groups of the membrane. This interaction can be an important factor affecting the membrane charge density, especially when multivalent ions, such as Ca^{2+} and Mg^{2+}, are present in solution [32–35]. Such interactions can even lead to reversal of the membrane charge and influence the transport properties of each individual ion [18,36].

The binding mechanism between polyamide functional groups and multivalent ions has previously been studied [37]. For instance, Thangaraj et al. already described how cations adsorb on polyamide resins and how PA acts as a polymeric chelate, adsorbing metal ions through a coordinate bond [38]. Bruni et al. developed a model for single salt solutions to describe competitive adsorption and site-binding of counterions in NF [34]. Similarly, Hall et al. studied and modeled a reverse osmosis process for a multi-electrolyte solution considering the adsorption of cations and their effect on the membrane charge density [36].

In Fig. 1, we illustrate the model problem of a multi-component electrolyte solution with three ions (Ca^{2+}, Na^{+}, and Cl^{-}). In this illustration, Ca^{2+} ions bind to negative carboxylic groups of the membrane. Therefore, when the concentration of Ca^{2+} is high enough, the surface charge of the membrane becomes positive (charge reversal), as we also show in Fig. 2.

In our model, we include the adsorption of cations in the membrane by describing the membrane charge density as function of the local cation concentration. We assume that only Ca^{2+} or Mg^{2+} ions can affect the membrane charge density. In addition, hindrance, membrane porosity, and pore tortuosity, are all included in a reduction factor for diffusion. It is the aim of the present study to show that mean-field theory (ENP) together with suitable models for ion adsorption, can accurately predict ion retention by NF membranes. Experimental data by Fridman et al. [39] and by Déon et al. [40] are used to evaluate the model. Besides, with the proposed model, we can explain some puzzling results, such as rejection of ions increasing with concentration or controlled by counterions, that previous models could not predict [31,39].

2. Theory

In the present section, we describe general theory, based on the extended Donnan steric partitioning pore model (ext-DSP model), to calculate the concentration difference that develops between the feed (influent solution) and the permeate (treated water) in NF. The ext-DSP model is based on the ENP equation, which includes advection, diffusion and electromigration, and in addition describes the partitioning of ions, Φ_i, between solution and membrane pores. Within this model, a Donnan balance applies at both edges of the membrane to include effects of steric hindrance and electric potential on the partitioning of ions. In the one-dimensional model proposed in this study, we only consider three types of ions, Cl^{-}, Na^{+}, and a divalent cation, either Ca^{2+} or Mg^{2+}, and neglect reactions between them [41] while we also neglect any involvement of H^{+} or OH^{-}. We include in the model how the membrane charge density is dependent on the adsorption of Ca^{2+} or Mg^{2+}. Only divalent cations are considered to adsorb to the negatively charged membrane groups, because they have a much stronger binding energy than monovalent cations.

The transport theory makes use of the ENP equation to describe the transport of ions through the membrane

$$J_i = v_F K_{c,i} c_i - K_{d,i} \varepsilon D_i \left(\frac{\partial c_i}{\partial x} + z_i c_i \frac{\partial \phi}{\partial x} \right) \tag{1}$$

where the ionic flux through the membrane, J_i, is a function of advection, diffusion and electromigration, respectively. The water velocity through the membrane is given by v_F, the factor $K_{c,i}$ accounts for a hindrance effect by which advection is reduced, and likewise $K_{d,i}$ is a reduction factor for diffusion and electromigration. The ion concentration in the membrane pores is given by c_i, D_i is the diffusion coefficient in bulk solution, ε is a reduction factor due to membrane porosity and tortuosity, and x is the coordinate across the membrane.

Inside the membrane, mass conservation of every ion, without chemical reactions, is given by

$$\frac{\partial c_i}{\partial t} = -\frac{\partial J_i}{\partial x} \tag{2}$$

which for steady-state can be combined with Eq. (1) to arrive at

$$0 = v_F K_{c,i} \frac{\partial c_i}{\partial x} - \zeta_i D_i \frac{\partial}{\partial x} \left(\frac{\partial c_i}{\partial x} + z_i c_i \frac{\partial \phi}{\partial x} \right) \tag{3}$$

where the reduction factor for diffusion ζ_i is given by $\zeta_i = K_{d,i} \cdot \varepsilon$. We solve Eq. (3) at each position x in the membrane, from the membrane-feed solution boundary, $x = 0$, to the membrane-permeate boundary, $x = \delta$, where δ refers to the thickness of the PA top layer. Besides, in relation to Eq. (3), we assume for all the ions the same hindrance factor for advection. In loose membranes, hindrances are less pronounced for advection than for diffusion, and $K_{c,i} \approx 1$ [42].

At both membrane-solution interfaces, we apply the Donnan equilibrium for each ion

$$c_i^* = c_{\text{out},i} \Phi_i e^{-z_i \Delta \phi_D} \tag{4}$$

where c_i^* is the ion concentration in the membrane at the membrane-feed solution boundary, or on the membrane-permeate boundary, and $c_{\text{out},i}$ is the corresponding concentration in solution just outside the membrane. At the edges of the membrane, the general ion partitioning coefficient, Φ_i, groups all the different phenomena that can affect the partitioning of ions. Since size exclusion is one of the main rejection mechanisms in membrane-based processes, the contribution of steric hindrances to the partitioning is often considered [43]. However, other phenomena can be included in the partitioning function to calculate Φ_i, e.g., dielectric exclusion [44], Born effect [45], and image forces [46]. In this study, we assume that the general partitioning coefficient, Φ_i, of all ions is the same to reduce the number of parameters in the model. The Donnan potential is given by $\Delta\phi_D$.

We consider local electroneutrality and zero electric current at all positions in the membrane, according to

$$\sum_i z_i c_i + X = 0 \tag{5}$$

and

$$\sum_i z_i J_i = 0 \tag{6}$$

where X is the charge density of the membrane, which can be constant, or can be variable. In that second case, X can depend on local concentrations, chemical interactions between ions and membrane material, and on acid-base reactions [28]. In this study, we make X a function of the local Ca^{2+} or Mg^{2+} concentration using the equations reported by Hall et al. [36], without including a direct effect of other ions. Even though Na^{+} might also interact with the negative carboxylic groups of the membrane, divalent cations have a stronger interaction and higher site-binding constant [47], which translates into a larger impact on the membrane charge density. Therefore, the membrane charge density is defined as function of the local concentration of divalent cations, c^{2+}, according to

$$X = X_0 \frac{1 - K_b \cdot c^{2+}}{1 + K_b \cdot c^{2+}} \tag{7}$$

with K_b the membrane-c^{2+} binding constant, and X_0 the bare membrane charge density, i.e., the charge in absence of divalent cations in solution. The derivation of this membrane charge model is explained in Section 1 of the Supporting Information (SI). In the charge model, we assume that

divalent cations bind to a single membrane group (1:1 interaction). This model allows the membrane charge to flip from negative, in the absence of divalent cations, to positive when sufficient numbers of divalent cations are present. An alternative membrane charge model is discussed in SI (Fig. S1), where we present results for the case when divalent cations bind to two membrane groups at the same time (1:2 interaction).

Another important variable is the rejection of ions, R_i, which is given by

$$R_i = 1 - \frac{c_{p,i}}{c_{f,i}} \tag{8}$$

where $c_{p,i}$ and $c_{f,i}$ are the concentration of ions in permeate and in feed.

In the model, we define a reference Peclet-number, $\mathrm{Pe}_{\mathrm{ref}} = \frac{\nu_F \delta}{D_{\mathrm{ref}}}$, where ν_F is the water velocity, δ is the membrane thickness, and D_{ref} is a reference diffusion coefficient. The Peclet-number is often used to express the ratio of transport by advection over transport by diffusion [48]. Nevertheless, defining a Peclet-number is also a convenient approach to non-dimensionalize transport equations [49]. In this work, we define a $\mathrm{Pe}_{\mathrm{ref}}$ to relate several parameters of the model mathematically. Especially for multi-component electrolyte solutions the definition of D_{ref} is very convenient, because we avoid defining specific Pe-numbers for each ion. Besides, with a $\mathrm{Pe}_{\mathrm{ref}}$, the transport model can be solved for any combination of ν_F and δ. Provided that the value of $\mathrm{Pe}_{\mathrm{ref}}$ is the same, the outcome of the transport model will not change.

3. Results and discussion

3.1. Membrane charge density

In this section, we study the effect of divalent cation adsorption on membrane charge density. The net membrane charge is the result of deprotonation or protonation of functional groups. In principle, two types of functional groups contribute to the membrane charge: the amide and carboxylic groups [43,50,51]. In acidic conditions (low pH, pH<5) the amide groups are mostly in protonated form ($[R-NH_2] + [H_3O^+] \rightleftharpoons [R-NH_3^+]$), while in alkaline condition (high pH, pH>7), the carboxylic groups are mostly in deprotonated form ($[R-COOH] \rightleftharpoons [R-COO^-] + [H_3O^+]$). Generally, when the solution pH is above pH = 5, polyamide composite membranes have a net negative surface charge ($X \approx [COO^-]$). However, for low pH conditions, the concentration of protonated amide groups must be included in the charge model ($X = [COO^-] + [NH_3^+]$). The charge model presented in this study can be easily extended to include the concentration of amide groups on the membrane charge density.

Fig. 2 depicts the results from the theoretical calculations of the membrane charge density, X, using parameters listed in Table 2, Case I, where the membrane charge density ranges from −400 to 400 mM. For a solution with low $[Ca^{2+}]_{\mathrm{feed}}$ the membrane is negatively charged (as low as $X = -400$ mM) but it becomes positively charged at a higher $[Ca^{2+}]_{\mathrm{feed}}$. The bare membrane charge density used in this model calculation, $X_0 = -400$ mM, falls in the range that has previously been reported for NF membranes [52–55].

One can identify three different effects of the presence of divalent cations on the membrane charge density, namely membrane charge screening, point of zero charge, and membrane charge reversal. Charge screening is the reduction of the membrane charge density without inversion of the sign. The point of zero charge (≈ 8 mM) represents the value of $[Ca^{2+}]_{\mathrm{feed}}$ that leads to a neutrally charged membrane. Charge reversal takes place after the point of zero charge, when $[Ca^{2+}]_{\mathrm{feed}}$ is higher than 8 mM. Moreover, $[Na^+]_{\mathrm{feed}}$ also influences charge screening and membrane charge reversal.

In Fig. 2, for 100 mM and 500 mM $[Na^+]_{\mathrm{feed}}$, the curve of charge density vs divalent cation concentration becomes quite steep when $[Ca^{2+}]_{\mathrm{feed}}$ increases to beyond 2.0 or 25 μM respectively, showing in that range a strong effect of the adsorption of counterions on the membrane charge density. For both solutions, 100 mM and 500 mM $[Na^+]_{\mathrm{feed}}$, at a concentration of 8 and 9 mM $[Ca^{2+}]_{\mathrm{feed}}$ respectively, the membrane charge is zero (point of zero charge). In practice, these concentrations are often reached and sometimes even higher [56,57], and thus membrane charge reversal must certainly be considered. Above the point of zero charge (8 or 9 mM), charge reversal takes place, with membrane charge density ultimately reaching $X = 400$ mM. The value of the binding constant, K_b, that we find in our study by fitting theory to the data, is comparable to values reported in literature [38].

Table 1
Transport parameters used in theory. Diffusion coefficients from Ref. [28].

$D_{\mathrm{ref}} = 1{\cdot}10^{-9}$ m^2/s	$D_{Mg^{2+}}/D_{\mathrm{ref}} = 0.706$	$\delta_{\mathrm{ref}} = 100$ nm
$D_{Na^+}/D_{\mathrm{ref}} = 1.334$	$D_{Ca^{2+}}/D_{\mathrm{ref}} = 0.791$	$K_{c,\,i} = 1$ for all ions
$D_{Cl^-}/D_{\mathrm{ref}} = 2.031$	$\mathrm{Pe}_{\mathrm{ref}} = 0.0015$	$\nu_F = 1.5$ μm/s

Table 2
Model parameters calculated to fit the experimental data for Case I based on Fridman et al. [39], and for Case II based on Déon et al. [40].

Case I		Case II	
X_0	−400 mM	X_0	−36 mM
K_b	2.28 mM^{-1}	K_b	1.57 mM^{-1}
Φ_{Cl^-}, Φ_{Na^+}, $\Phi_{Ca^{2+}}$	0.19	Φ_{Cl^-}, Φ_{Na^+}, $\Phi_{Mg^{2+}}$	0.13
ζ_{Cl^-}	0.0046	ζ_{Cl^-}	0.0077
ζ_{Na^+}	0.0314	ζ_{Na^+}	0.0277
$\zeta_{Ca^{2+}}$	0.0143	$\zeta_{Mg^{2+}}$	0.0014

3.2. Model predictions

In this section we compare our model outcome with experimental data. In Table 1, the general transport parameters used are reported. The Nelder-Mead method [58] was used to find model parameters that make the theory fit closely to data from two studies [39,40]. Detailed information about the Nelder-Mead procedure is given in Section 3 of SI. The Nelder-Mead procedure was successful and gave us a good fit of the theory to experimental data, and provided realistic parameter settings that we report in Table 2. Interestingly, the reduction of diffusion for divalent cations is lower than for monovalent cations ($\zeta_{Na^+} > \zeta_{Ca^{2+}}$ and $\zeta_{Mg^{2+}}$), which agrees with the results from Shefer et al. [59]

The data from Fridman et al. [39] was the first set of data used to develop and evaluate the model. The description of the experimental protocol is summarized in SI. These data correspond to two solutions with a total feed Cl^- concentration, $[Cl^-]_{\mathrm{tot}}$, of 100 mM and of 500 mM, while the concentration of cations was varied. The equivalent Na^+ fraction in the feed, θ, is defined as

$$\theta = \frac{[\mathrm{NaCl}]_{\mathrm{feed}}}{[Cl^-]_{\mathrm{tot}}} = \frac{[\mathrm{NaCl}]_{\mathrm{feed}}}{[\mathrm{NaCl}]_{\mathrm{feed}} + 2{\cdot}[\mathrm{CaCl_2}]_{\mathrm{feed}}}. \tag{9}$$

In Fig. 3, we show experimental data and model predictions for the rejection of Na^+ (Fig. 3a) and Ca^{2+} (Fig. 3b) as function of feed composition, θ. Blue and red lines are our model predictions that considers Ca^{2+} adsorption on the membrane. The grey dashed line shows an earlier calculation result by Fridman et al. for $[Cl^-]_{\mathrm{tot}} = 100$ mM [39], in which adsorption of Ca^{2+} ions to the membrane was not considered.

Including the effect of Ca^{2+} ions on the membrane charge density leads to a better prediction of the experimental data. Fig. 3 depicts the effect of Ca^{2+} concentration on the rejection of cations, i.e., increased concentrations of Ca^{2+} in the feed solution results in increased rejection of Ca^{2+}. The charge reversal phenomenon can explain these results. With Ca^{2+} concentrations above 8 mM the membrane is positively charged (Fig. 2), and therefore the rejection of divalent cations is enhanced due to electrostatic repulsion.

Fig. 3a depicts how Na^+ rejection decreases to negative values, when its concentration in the feed is less than $\theta \sim 0.4$. This special situation

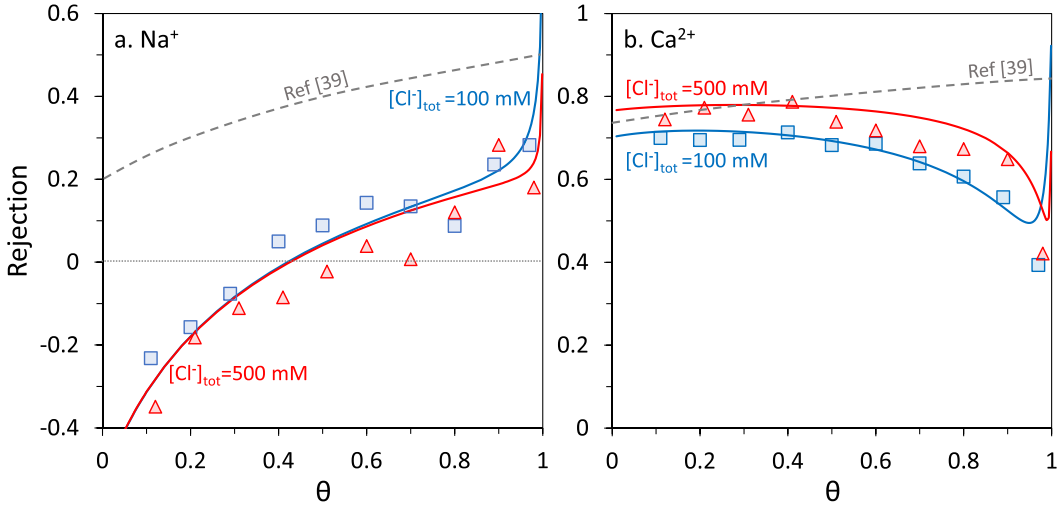

Fig. 3. Rejection as function of feed compositions, θ, and $[Cl^-]_{tot}$ of a) Na^+ and b) Ca^{2+} by NF membrane NF270. Blue and red lines are our model predictions, the grey dashed line is the prediction by Fridman et al, and symbols are experimental data [39]. Model parameters are in Table 2, Case I.

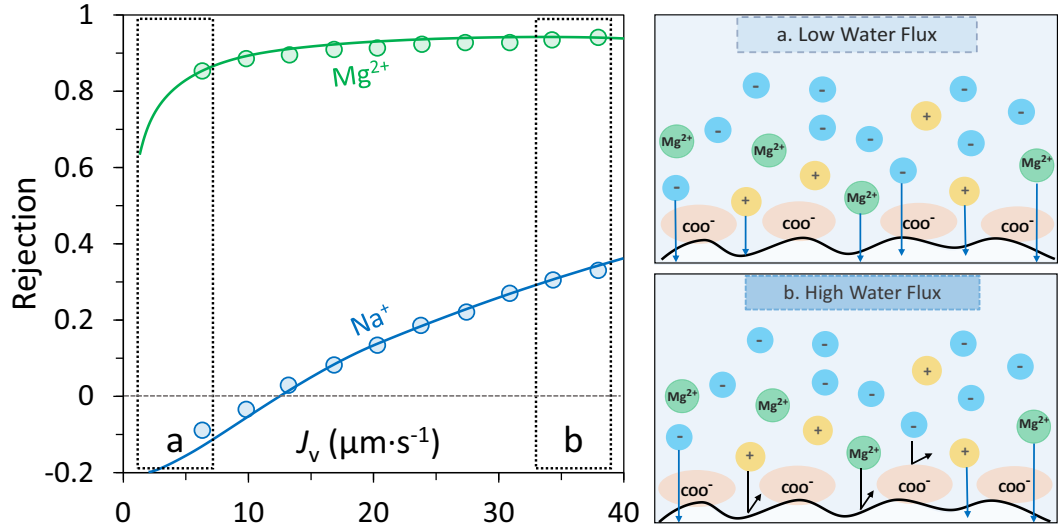

Fig. 4. Ion rejection by NF membranes from solution with monovalent and divalent cations as function of permeate flux, J_v. Lines are theory and symbols are experimental data from Déon et al. ($[Cl^-]_{tot}$=100 mM). Model parameters in Table 2, Case II [40].

will be discussed in Section 3.3.1. In contrast, Fig. 3b shows how Ca^{2+} rejection is relatively stable and only at very low $[Ca^{2+}]_{feed}$, i.e., high θ, drops off, in agreement with ref. [60] This steep decay in rejection of Ca^{2+} at high θ is found both in theory and experiments. As expected for NF, the rejection of divalent ions is much higher than of monovalent ions. Comparing this result with the model prediction by Fridman et al. [39] (grey dashed line) shows that including the adsorption of Ca^{2+} ions to the membrane significantly improves the prediction of ion rejection. Therefore, contrary to what is reported in literature [31], in this study we conclusively demonstrate that it is possible to rationalize the puzzling behavior (e.g., rejection of ions increasing with concentration or controlled by counterions) of three ions in solution by using a model based on the extended Nernst-Planck equation (mean-field theory) in which the adsorption of counterions in the membrane is included.

In a second exercise, we analyzed experimental data from a second study to further validate our model [40]. In this second study, ternary ion mixtures were tested with different membranes and experimental conditions. We analyze their data, for one membrane (AFC40), tested with a ternary salt mixture of Na^+, Mg^{2+}, and Cl^-. We used data reported for a solution of 50 mM Na^+ and 25 mM Mg^{2+} feed concentration. Despite the different membranes and the use of Mg^{2+} instead of Ca^{2+}, the principle of cation binding to the carboxylic groups of the polyamide layer is expected to be the same. Mg^{2+} ions have shown similar ion-surface interactions that can lead to charge reversal [61].

By using the value of membrane charge density reported by Déon et al. [40] and calculating the binding constant, K_b, and the values of the reduction factors for diffusion, ζ_i, for each ion, we can again reproduce the data of ion rejection. For this case, the general transport parameters are given in Table 1, and the values of the model parameters are reported in Table 2, Case II. Fig. 4 depicts the experimental data [40] and model predictions for the rejection of Mg^{2+} and Na^+ as function of the permeate flux J_v, which is equivalent to the water velocity through the membrane, v_F.

The gradual increase of ion rejection with water flux is clearly shown. In this data set, the rejection of divalent cations is higher than of monovalent cations, which is attributed to the effect of Mg^{2+} on the membrane charge density. Besides, negative rejections for Na^+ are observed again, now at low water flux, which are perfectly reproduced by our model. Indeed, the accurate reproduction of these experimental data with our model shows again that the adsorption of divalent cations

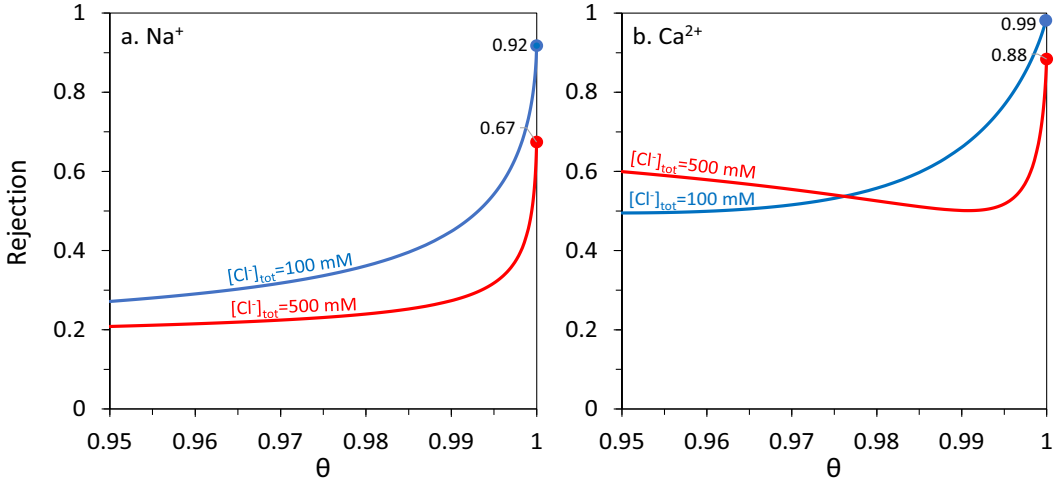

Fig. 5. Close-up of theoretical results of Fig. 3 in the limit close to θ=1.

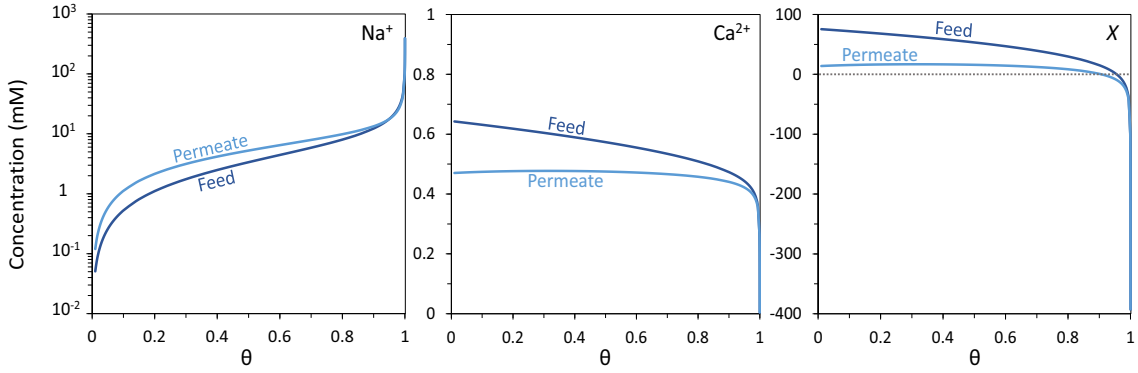

Fig. 6. Predicted concentration of Na^+ and Ca^{2+}, in the membrane, at the two interfaces, as well as membrane charge density, X, at these two locations.

in the membrane is an important element in theoretical descriptions of NF.

3.3. Analysis

3.3.1. Limiting cases

There are two interesting situations in the limits of $\theta \sim 0$ and $\theta \sim 1$ in Fig. 3a and b. In the first region, when $\theta \sim 0$, the model and the experimental data show a rejection below zero, $R_{Na^+} < 0$, which can be considered a quite unexpected result. However, this situation has already been reported in literature, especially for multi-component electrolyte solutions in the presence of multivalent ions [35,62–66]. Yaroshchuk et al. studied the different cases and reasons behind the negative rejection [67]. The membrane properties (e.g., charge and material), the ions in the solution and the operating conditions are some of the parameters that can lead to $R_i<0$. In this particular case, when a counterion with lower valence (Na^+) is a trace ion and a highly charged membrane is used, the electroneutrality principle is the main reason for $R_i<0$. When multiple counterions with different mobilities and valencies are in solution, due to the electric field, the counterion with a single charge is accelerated, especially when there is a low passage of multivalent ions through the membrane.

The second limit is in the region close to θ= 1. This limit is illustrated in Fig. 5, which is a magnification of Fig. 3a and b. Blue and red lines represent the case for $[Cl^-]_{tot}$ of 100 mM and 500 mM, respectively. In this region, there is a sharp increase in the rejection of both ions, R_{Na^+} and $R_{Ca^{2+}}$. To explain the increase in $R_{Ca^{2+}}$, we need to consider that, in this region, Ca^{2+} is present as a trace ion. When a trace ion has a higher charge, and its sign is the same as the faster dominant ion, there is an increase in the rejection of the trace ion [68].

On the other hand, there are no effects of the trace ion on the membrane characteristics and on the transport mechanisms of the dominant ions [69]. Thus, the membrane charge density is not affected and the co-ion, in this case Cl^-, determines the rejection. The lower the Ca^{2+} concentration in the feed, the more negative the membrane charge density and the lower the Cl^- concentration inside the membrane, which limits the transport of both Cl^- and Na^+ due to the zero current principle as summarized in Eq. (6).

3.3.2. Concentration profiles across the membrane

Now, we present and discuss the concentrations of Na^+ and Ca^{2+}, and the membrane charge density, X, just inside the membrane, at both membrane interfaces, as function of θ, for $[Cl^-]_{tot}$ = 100 mM.

Fig. 6 shows that the concentrations of ions, and the membrane charge density, are different between the two sides of the membrane. For instance, the concentration of Ca^{2+} gradually decreases across the membrane, from the feed to the permeate side, and this has the expected effect to lower the membrane charge density. On the other hand, the concentration of Na^+ increases across the membrane. For both cations, the difference in concentration across the membrane is largest for low values of θ (Na^+ trace condition). This result is in agreement with the analysis of negative rejections of Na^+ given in Section 3.3.1.

4. Conclusions

The ability to better reject divalent ions over monovalent ions makes NF suitable for interesting engineering and environmental science applications, including water reclamation, water softening, and desalination. For a wide range of NF applications, it is important to be able to predict ion rejection accurately. In this study, we focused on multi-component electrolyte solution with three ions: Na^+, Ca^{2+} (or Mg^{2+}), and Cl^-. Such a multi-component electrolyte solution is expected to show discrepancies between theory and experimental data and an unexpected behavior compared to single salt solutions. However, this study shows that mean-field theory can be adapted to include important physicochemical phenomena and explain such unexpected results. Moreover, the results of this study highlight the importance of considering the interaction between counterions and the charged functional groups of the membrane. In some cases, counterion binding to the membrane can lead to charge reversal, which completely affects the rejection of all the ions. Finally, this work opens up the possibility for future studies to consider interactions between ions (e.g., Na^+, Ca^{2+}, and Mg^{2+}) and the active layer of the membrane.

CRediT authorship contribution statement

The manuscript was written through contributions of all authors. All authors have given approval to the final version of the manuscript.

Declaration of competing interest

The authors declare that they have no known competing financial interests or personal relationships that could have appeared to influence the work reported in this paper.

Acknowledgement

This work was performed in the cooperation framework of Wetsus, European Centre of Excellence for Sustainable Water Technology (www.wetsus.nl). Wetsus is co-funded by the Dutch Ministry of Economic Affairs and Ministry of Infrastructure and Environment, the European Union Regional Development Fund, the Province of Fryslân and the Northern Netherlands Provinces. This work is part of a project that has received funding from the European Union's Horizon 2020 research and innovation programme under the Marie Skłodowska-Curie grant agreement No 665874.

Appendix A. Supplementary data

Supporting Information. Adsorption model, c^{2+}-carboxyl interaction, Nelder-Mead calculation. Supplementary data to this article can be found online at https://doi.org/10.1016/j.desal.2022.115552

References

[1] N. Hilal, H. Al-Zoubi, A.W. Mohammad, N. Darwish, Nanofiltration of highly concentrated salt solutions up to seawater salinity, Desalination 184 (2005) 315–326.
[2] L. Llenas, X. Martnez-Lladó, A. Yaroshchuk, M. Rovira, J. de Pablo, Nanofiltration as pretreatment for scale prevention in seawater reverse osmosis desalination, Desalin. Water Treat. 36 (2011) 310–318.
[3] E. Virga, J. de Grooth, K. Žvab, W.M. de Vos, Stable polyelectrolyte multilayer-based hollow fiber nanofiltration membranes for produced water treatment, ACS Appl. Polym. Mater. 1 (2019) 2230–2239.
[4] B. van der Bruggen, I. De Vreese, C. Vandecasteele, Water reclamation in the textile industry: nanofiltration of dye baths for wool dyeing, Ind. Eng. Chem. Res. 40 (2001) 3973–3978.
[5] E. Sahinkaya, N. Uzal, U. Yetis, F.B. Dilek, Biological treatment and nanofiltration of denim textile wastewater for reuse, J. Hazard. Mater. 153 (2008) 1142–1148.
[6] Y.K. Ong, F.Y. Li, S.-P. Sun, B.-W. Zhao, C.-Z. Liang, T.-S. Chung, Nanofiltration hollow fiber membranes for textile wastewater treatment: lab-scale and pilot-scale studies, Chem. Eng. Sci. 114 (2014) 51–57.
[7] R. Castro-Muñoz, Pressure-driven membrane processes involved in waste management in agro-food industries: a viewpoint, AIMS Energy 6 (2018) 1025–1031.
[8] B. van der Bruggen, C. Vandecasteele, Removal of pollutants from surface water and groundwater by nanofiltration: overview of possible applications in the drinking water industry, Environ. Pollut. 122 (2003) 435–445.
[9] K. Košutić, L. Furač, L. Sipos, B. Kunst, Removal of arsenic and pesticides from drinking water by nanofiltration membranes, Sep. Purif. Technol. 42 (2005) 137–144.
[10] K. Pan, Q. Song, L. Wang, B. Cao, A study of demineralization of whey by nanofiltration membrane, Desalination 267 (2011) 217–221.
[11] P. Chen, X. Ma, Z. Zhong, F. Zhang, W. Xing, Y. Fan, Performance of ceramic nanofiltration membrane for desalination of dye solutions containing NaCl and NaSO, Desalination 404 (2017) 102–111.
[12] M. Park, J. Park, E. Lee, J. Khim, J. Cho, Application of nanofiltration pretreatment to remove divalent ions for economical seawater reverse osmosis desalination, Desalin. Water Treat. 57 (2016) 20661–20670.
[13] A. Figoli, A. Criscuoli, Sustainable Membrane Technology for Water and Wastewater Treatment, Springer, 2017.
[14] A.F. Ismail, M. Padaki, N. Hilal, T. Matsuura, W.J. Lau, Thin film composite membraneâ€"Recent development and future potential, Desalination 356 (2015) 140–148.
[15] D.L. Oatley, L. Llenas, R. Pérez, P.M. Williams, X. Martnez-Lladó, M. Rovira, Review of the dielectric properties of nanofiltration membranes and verification of the single oriented layer approximation, Adv. Colloid Interface Sci. 173 (2012) 1–11.
[16] M. Mänttäri, A. Pihlajamäki, M. Nyström, Effect of pH on hydrophilicity and charge and their effect on the filtration efficiency of NF membranes at different pH, J. Membr. Sci. 280 (2006) 311–320.
[17] A. Schaefer, A.G. Fane, T.D. Waite, Nanofiltration: Principles and Applications, Elsevier, 2005.
[18] M.R. Teixeira, M.J. Rosa, M. Nyström, The role of membrane charge on nanofiltration performance, J. Membr. Sci. 265 (2005) 160–166.
[19] A.W. Mohammad, Y.H. Teow, W.L. Ang, Y.T. Chung, D.L. Oatley-Radcliffe, N. Hilal, Nanofiltration membranes review: recent advances and future prospects, Desalination 356 (2015) 226–254.
[20] P.M. Biesheuvel, J.E. Dykstra, Physics of Electrochemical Processes, 2020.
[21] L. Dresner, Stability of the extended nernst-planck equations in the description of hyperfiltration through ion-exchange membranes, J. Phys. Chem. 76 (1972) 2256–2267.
[22] A. Yaroshchuk, M.L. Bruening, E. Zholkovskiy, Modelling nanofiltration of electrolyte solutions, Adv. Colloid Interface Sci. 268 (2019) 39–63.
[23] R. Wang, S. Lin, Pore model for nanofiltration: history, theoretical framework, key predictions, limitations, and prospects, J. Membr. Sci. 620 (2020), 118809.
[24] J. Schaep, C. Vandecasteele, A.W. Mohammad, W.R. Bowen, Modelling the retention of ionic components for different nanofiltration membranes, Sep. Purif. Technol. 22 (2001) 169–179.
[25] B. Saliha, F. Patrick, S. Anthony, Investigating nanofiltration of multi-ionic solutions using the steric, electric and dielectric exclusion model, Chem. Eng. Sci. 64 (2009) 3789–3798.
[26] J.M.M. Peeters, J.P. Boom, M.H.V. Mulder, H. Strathmann, Retention measurements of nanofiltration membranes with electrolyte solutions, J. Membr. Sci. 145 (1998) 199–209.
[27] T. Urase, J.-I. Oh, K. Yamamoto, Effect of pH on rejection of different species of arsenic by nanofiltration, Desalination 117 (1998) 11–18.
[28] P.M. Biesheuvel, L. Zhang, P. Gasquet, B. Blankert, M. Elimelech, W.G.J. van der Meer, Ion selectivity in brackish water desalination by reverse osmosis: theory, measurements, and implications, Environ. Sci. Technol. Lett. 7 (2019) 42–47.
[29] N. Fridman-Bishop, O. Nir, O. Lahav, V. Freger, Predicting the rejection of major seawater ions by spiral-wound nanofiltration membranes, Environ. Sci. Technol. 49 (2015) 8631–8638.
[30] S. Bason, V. Freger, Phenomenological analysis of transport of mono-and divalent ions in nanofiltration, J. Membr. Sci. 360 (2010) 389–396.
[31] V. Freger, Ion partitioning and permeation in charged low- membranes, Adv. Colloid Interface Sci. 277 (2020), 102107.
[32] J. Schaep, C. Vandecasteele, A.W. Mohammad, W.R. Bowen, Analysis of the salt retention of nanofiltration membranes using the donnan-steric partitioning pore model, Sep. Sci. Technol. 34 (1999) 3009–3030.
[33] S. Déon, A. Escoda, P. Fievet, A transport model considering charge adsorption inside pores to describe salts rejection by nanofiltration membranes, Chem. Eng. Sci. 66 (2011) 2823–2832.
[34] L. Bruni, S. Bandini, Studies on the role of site-binding and competitive adsorption in determining the charge of nanofiltration membranes, Desalination 241 (2009) 315–330.
[35] J. Garcia-Aleman, J.M. Dickson, Permeation of mixed-salt solutions with commercial and pore-filled nanofiltration membranes: membrane charge inversion phenomena, J. Membr. Sci. 239 (2004) 163–172.
[36] M.S. Hall, V.M. Starov, D.R. Lloyd, Reverse osmosis of multicomponent electrolyte solutions part I. Theoretical development, J. Membr. Sci. 128 (1997) 23–37.
[37] W.M. de Vos, S. Lindhoud, Overcharging and charge inversion: finding the correct explanation(s), Adv. Colloid Interf. Sci. 274 (2019), 102040.
[38] V. Thangaraj, K. Aravamudan, R. Lingam, S. Subramanian, Individual and simultaneous adsorption of ni (II), cd (II), and zn (II) ions over polyamide resin: equilibrium, kinetic and thermodynamic studies, Environ. Prog. Sustain. Energy 38 (2019) S340–S351.

[39] N. Fridman-Bishop, K.A. Tankus, V. Freger, Permeation mechanism and interplay between ions in nanofiltration, J. Membr. Sci. 548 (2018) 449–458.
[40] S. Déon, A. Escoda, P. Fievet, P. Dutournié, P. Bourseau, How to use a multi-ionic transport model to fully predict rejection of mineral salts by nanofiltration membranes, Chem. Eng. J. 189 (2012) 24–31.
[41] E.M. Kimani, A.J.B. Kemperman, W.G.J. van der Meer, P.M. Biesheuvel, Multicomponent mass transport modeling of water desalination by reverse osmosis including ion pair formation, J. Chem. Phys. 154 (2021), 124501.
[42] P. Dechadilok, W.M. Deen, Hindrance factors for diffusion and convection in pores, Ind. Eng. Chem. Res. 45 (2006) 6953–6959.
[43] Y.S. Oren, P.M. Biesheuvel, Theory of ion and water transport in reverse-osmosis membranes, Phys. Rev. Appl. 9 (2018), 024034.
[44] A.G. Guzmán-Garcia, P.N. Pintauro, M.W. Verbrugge, R.F. Hill, Development of a space-charge transport model for ion-exchange membranes, AICHE J. 36 (1990) 1061–1074.
[45] D.L. Oatley, L. Llenas, N.H. Aljohani, P.M. Williams, X. Martnez-Lladó, M. Rovira, J. de Pablo, Investigation of the dielectric properties of nanofiltration membranes, Desalination 315 (2013) 100–106.
[46] A. Szymczyk, P. Fievet, Investigating transport properties of nanofiltration membranes by means of a steric, electric and dielectric exclusion model, J. Membr. Sci. 252 (2005) 77–88.
[47] L. Bruni, S. Bandini, The role of the electrolyte on the mechanism of charge formation in polyamide nanofiltration membranes, J. Membr. Sci. 308 (2008) 136–151.
[48] M. Huysmans, A. Dassargues, Review of the use of Péclet numbers to determine the relative importance of advection and diffusion in low permeability environments, Hydrogeol. J. 13 (2005) 895–904.
[49] B.E. Rapp, Microfluidics: Modeling, Mechanics and Mathematics, William Andrew, 2016.
[50] O. Coronell, M.I. González, B.J. Mariñas, D.G. Cahill, Ionization behavior, stoichiometry of association, and accessibility of functional groups in the active layers of reverse osmosis and nanofiltration membranes, Environ. Sci. Technol. 44 (2010) 6808–6814.
[51] S. Bandini, C. Mazzoni, Modelling the amphoteric behaviour of polyamide nanofiltration membranes, Desalination 184 (2005) 327–336.
[52] C. Labbez, P. Fievet, A. Szymczyk, A. Vidonne, A. Foissy, J. Pagetti, Retention of mineral salts by a polyamide nanofiltration membrane, Sep. Purif. Technol. 30 (2003) 47–55.
[53] S. Ong, W. Zhou, L. Song, W. Ng, Evaluation of feed concentration effects on salt/ion transport through RO/NF membranes with the nernst-planck-donnan model, Environ. Eng. Sci. 19 (2002) 429–439.
[54] G. Artuğ, I. Roosmasari, K. Richau, J. Hapke, A comprehensive characterization of commercial nanofiltration membranes, Sep. Sci. Technol. 42 (2007) 2947–2986.
[55] A. Mohammad, N. Hilal, H. Al-Zoubi, N. Darwish, Prediction of permeate fluxes and rejections of highly concentrated salts in nanofiltration membranes, J. Membr. Sci. 289 (2007) 40–50.
[56] M. Vourch, B. Balannec, B. Chaufer, G. Dorange, Treatment of dairy industry wastewater by reverse osmosis for water reuse, Desalination 219 (2008) 190–202.
[57] Y.A. Le Gouellec, M. Elimelech, Calcium sulfate (gypsum) scaling in nanofiltration of agricultural drainage water, J. Membr. Sci. 205 (2002) 279–291.
[58] J.A. Nelder, R. Mead, A simplex method for function minimization, Comput. J. 7 (1965) 308–313.
[59] I. Shefer, O. Peer-Haim, O. Leifman, R. Epsztein, Enthalpic and entropic selectivity of water and small ions in polyamide membranes, Environ. Sci. Technol. 55 (2021) 14863–14875.
[60] C. Mazzoni, S. Bandini, On nanofiltration Desal-5 DK performances with calcium chloride–water solutions, Sep. Purif. Technol. 52 (2006) 232–240.
[61] S.X. Li, W. Guan, B. Weiner, M.A. Reed, Direct observation of charge inversion in divalent nanofluidic devices, Nano Lett. 15 (2015) 5046–5051.
[62] G. Hagmeyer, R. Gimbel, Modelling the salt rejection of nanofiltration membranes for ternary ion mixtures and for single salts at different pH values, Desalination 117 (1998) 247–256.
[63] K. Linde, A.-S. Jönsson, Nanofiltration of salt solutions and landfill leachate, Desalination 103 (1995) 223–232.
[64] J. Tanninen, M. Nyström, Separation of ions in acidic conditions using NF, Desalination 147 (2002) 295–299.
[65] T. Tsuru, M. Urairi, S. Nakao, S. Kimura, Reverse osmosis of single and mixed electrolytes with charged membranes: experiment and analysis, J. Chem. Eng. Jpn 24 (1991) 518–524.
[66] N. Pagès, M. Reig, O. Gibert, J.L. Cortina, Trace ions rejection tunning in NF by selecting solution composition: ion permeances estimation, Chem. Eng. J. 308 (2017) 126–134.
[67] A.E. Yaroshchuk, Negative rejection of ions in pressure-driven membrane processes, Adv. Colloid Interf. Sci. 139 (2008) 150–173.
[68] A. Yaroshchuk, X. Martnez-Lladó, L. Llenas, M. Rovira, J. de Pablo, Solution-diffusion-film model for the description of pressure-driven trans-membrane transfer of electrolyte mixtures: one dominant salt and trace ions, J. Membr. Sci. 368 (2011) 192–201.
[69] N. Pages, A. Yaroshchuk, O. Gibert, J.L. Cortina, Rejection of trace ionic solutes in nanofiltration: influence of aqueous phase composition, Chem. Eng. Sci. 104 (2013) 1107–1115.